

Distance and intersection number in the curve graph of a surface

Joan Birman*, Matthew J. Morse, and Nancy C. Wrinkle

March 7, 2019

Abstract

In this work, we study the cellular decomposition of S induced by a filling pair of curves v and w , $Dec_{v,w}(S) = S \setminus (v \cup w)$, and its connection to the distance function $d(v, w)$ in the curve graph of a closed orientable surface S of genus g . Efficient geodesics were introduced by the first author in joint work with Margalit and Menasco in 2016, giving an algorithm that begins with a pair of non-separating filling curves that determine vertices (v, w) in the curve graph of a closed orientable surface S and computing from them a finite set of *efficient* geodesics. We extend the tools of efficient geodesics to study the relationship between distance $d(v, w)$, intersection number $i(v, w)$, and $Dec_{v,w}(S)$. The main result is the development and analysis of particular configurations of rectangles in $Dec_{v,w}(S)$ called *spirals*. We are able to show that, in some special cases, the efficient geodesic algorithm can be used to build an algorithm that reduces $i(v, w)$ while preserving $d(v, w)$. At the end of the paper, we note a connection of our work to the notion of extending geodesics.

1 Introduction

The *curve graph* $\mathcal{C}(S)$ of a closed orientable surface $S = S_g$ of genus $g \geq 2$ is the metric graph whose vertices correspond to isotopy classes of essential simple closed curves in S . Edges join vertices that have disjoint representatives in S . Each edge is defined to have length 1. Let v, w be vertices in $\mathcal{C}(S)$. The *distance* $d(v, w)$ is the length of a shortest path in the curve graph from v to w . Any shortest path is a *geodesic* from v to w in $\mathcal{C}(S)$.

In 2002, the PhD thesis of Jason Leasure [Lea] presented an algorithm to compute the exact distance between two vertices of $\mathcal{C}(S)$, noting that there was no hope of implementing his algorithm for concrete computations. Fourteen years later Birman, Margalit and Menasco [BMM] produced a much faster algorithm of a similar spirit as that of [Lea] and was implemented as a computer program [MICC], which supplied new data for low distances and low genus. Our work in this paper was inspired by a desire to use the data provided by [MICC] to begin to create a bridge between the newly available tools in [BMM] and the mainstream work of the past 20 years on the large-scale geometry of the curve graph (starting with [MM-I], [MM-II].)

With that goal in mind we assume, as in [BMM], that vertices in the curve graph are isotopy classes of *non-separating* curves on the surface S (see [BM] for the underlying reasons for this assumption, and see [Ras] for a review of properties of the non-separating curve graph.)

*Supported partially by a Simons Foundation Collaborative Research Grant

We assume further that paths in the curve graph $\mathcal{C}(S)$ that join vertices are always chosen to be *efficient* in the sense of [BMM]. We will follow the conventions of the literature in abusing notation to denote vertices in the curve graph $\mathcal{C}(S)$ as well as representative curves in each isotopy class by v, w . It will be clear from context when v is a curve or an isotopy class of curves. We assume that each region $S \setminus v \cup w$ is a topological disc; such a v and w are a *filling pair* and are said to *fill* S . This condition implies that $d(v, w) \geq 3$. In addition, we assume that v and w are in *minimal position*: $|v \cap w|$ is minimized with respect to the isotopy classes of v and w . This implies that there are no bigons. We then define the intersection number of v and w , $i(v, w) = |v \cap w|$. Let $i_{\min}(d, g)$, or i_{\min} if there is no ambiguity, denote the minimal intersection number possible for all choices of vertices $v, w \in \mathcal{C}(S)$ having distance d on the surface S_g . We will refine this definition below.

Much of the work of this paper is based on studying the result of cutting S open along v and w ($S \setminus (v \cup w)$), which we refer to as the *decomposition of S by $v \cup w$* or just the *decomposition of v and w* and denote by $Dec_{v,w}(S)$. Since we assume the curves fill S , we know that $Dec_{v,w}(S)$ is a union of discs. Each disc is isotopic to a polygon with alternating edges in v and w . We observe that each polygon has an even number of total sides. $Dec_{v,w}(S)$ consists of more than a simple list of polygons of various sizes, however. $Dec_{v,w}(S)$ should also keep track of how the cut-open curves are identified to reform the surface, so along with the polygons themselves we include the polygonal edge identifications, which means two copies of labels $1, 2, \dots, i(v, w)$ and $1', 2', \dots, i(v, w)'$, one for each copy of v and w . We note that this identification is also guided by the fact that our surface is orientable: we are gluing polygons together so that the “positive” sides of the surface face out. Note that, while vertices are not oriented curves, our labeling requires an arbitrary choice of orientation. This choice does not affect any subsequent results.

See Figure 1 for an example of the cut-open surface, with the w -edges of the polygons identified. Here we see that there are sequences, or *bands*, of 4-gons connecting the 6-gons. These bands play a critical role in the results of this paper.

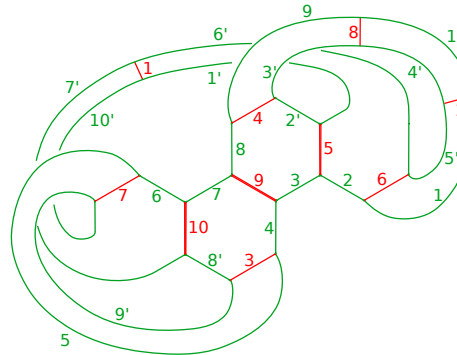


Figure 1: $S - v$ with edges of w identified. Here $g = 2, i = 10$, and $d = 3$ (distance verified by MICC.)

Let F_{2k} be the number of polygons in $Dec_{v,w}(S)$ with $2k$ sides, for $k \geq 2$ (because there are no bigons). We will refer to such polygons as *2k-gons*; when $k = 2$, such polygons are referred to as *4-gons* or *rectangles*. We call the vector of the numbers of each size of polygon the *decomposition vector* $\{F_6, F_8, \dots, F_{2k}, \dots, F_{8g-4}\}$. We will derive in §2.1 that the length of this vector is $4g - 4$. Two decompositions are *equivalent* if they have the same decomposition vector and the labels on v and/or w differ by a cyclic permutation. In this paper, we use a refined definition of i_{\min} ; that is, the minimal intersection number for two curves of fixed distance d in the curve graph of a surface of genus g such that their decomposition is in a given

equivalence class of decompositions.

The main results of this paper (in §3 and §4) are for decompositions consisting of 4-gons and 6-gons only. Before restricting our attention to this special case, we will make some general observations about $Dec_{v,w}(S)$.

Recall the well-known upper bound for the distance $d(v, w)$ that is attributed to Lickorish, but was first stated by Hempel in [He], relating distance and intersection number:

$$d(v, w) \leq 2 \log_2(i(v, w)) + 2 \quad (1)$$

This inequality can be interpreted in a new way, which we now explain. Euler characteristic considerations in §2.1 show that:

$$4g - 4 = F_6 + 2F_8 + 3F_{10} + \cdots + (4g - 4)F_{8g-4} \quad (2)$$

Equation (2) tells us that there are finitely many possibilities for the decomposition of S into polygons larger than rectangles. Note that the number F_4 of rectangles does not appear in (2). We will show (see §2.1 below) that:

$$i(v, w) = F_4 + \mathcal{F}_g, \text{ where } \mathcal{F}_g = (1/2)(3F_6 + 4F_8 + \cdots + (4g - 2)F_{8g-4}) \quad (3)$$

When combined with the inequality in Equation (1), we get our first connection between distance and decomposition:

$$d(v, w) \leq 2 \log_2(F_4 + \mathcal{F}_g) + 2. \quad (4)$$

Since we have finitely many possibilities for \mathcal{F}_g , the parameter F_4 in (4) plays the role of $i(v, w)$ in (1); therefore $i(v, w) \rightarrow \infty$ implies that $F_4 \rightarrow \infty$. Given this relationship between intersection number and rectangles, our primary effort in this paper is to provide an algorithm that, a given pair of vertices (v, w) , produces a new pair (v', w') with lower intersection number by reducing F_4 , while preserving both \mathcal{F}_g and the distance $d(v, w)$.

In the context of (4), observe that the problem of minimizing $i(v, w)$ or F_4 , while preserving \mathcal{F}_g and $d(v, w)$, goes hand in hand with the problem of increasing F_4 and increasing $d(v, w)$ while preserving \mathcal{F}_g . This is because one must understand how to recognize when $d(v, w)$ decreases as we reduce F_4 . Thus, we will be implicitly studying the growth of $d(v, w)$ as F_4 increases as we study the reduction of F_4 and preservation of $d(v, w)$. We discuss this connection further in §5.

Much of this work was motivated by studying a wealth of low-distance examples provided by the program MICC (Metric in the Curve Complex), which partially implements the efficient geodesic algorithm of [BMM]. The paper [GMM] explains the program and the results derived from it; the program itself is available for free download at [MICC]. MICC takes as its input two curves v, w and computes various associated properties: the genus of the surface S they lie on, the distance between v and w in the curve graph $\mathcal{C}(S)$, the number and types of polygons comprising $Dec_{v,w}(S)$, how those polygons are glued together to recover S , and information about the efficient geodesics between the two curves (see Section 4.1 for information on how this input is coded). Although the data we studied from MICC are very specific ($g = 2$, $d(v, w) \geq 4$), there is insight to be gained from further investigation there. The data produced by MICC in [GMM] was mainly for the case $g = 2$ and $d = 3$ and 4, with incomplete data for $g = 3, d = 4$. However, upon further inspection of these examples, we discovered that, for small $i(v, w)$, the possible face decompositions depend strongly on intersection number.

The important property of the data set for this work is that it contained all isotopy classes of distance ≥ 4 with $i(v, w) \leq 25$ and genus $g = 2$. The reasonable size of the examples

enabled rapid experimentation and verification of calculations, and the completeness of the data allowed us to make conclusions about $d(v, w)$ with respect to $Dec_{v,w}(S)$. The key observation from the data that is relevant to this work is that the minimum intersection number $i_{min}(d, g) = i_{min}(4, 2) = 12$ is not always realizable for a given decomposition vector describing $Dec_{v,w}(S)$. To be precise, for genus 2 surfaces and distance 4 curve pairs, if $(F_6, F_8, F_{10}, F_{12}) = (0,0,0,1)$ or $(1,0,1,0)$, then the minimum intersection number for v and w is > 12 . However, if $(F_6, F_8, F_{10}, F_{12}) = (4,0,0,0)$, $(2,1,0,0)$ or $(0,2,0,0)$, then $i_{min} = 12$. This indicates a clear dependence of $d(v, w)$ on $Dec_{v,w}(S)$.

It is known from the work of Aougab and Taylor [AT] that at ‘large’ distances the minimum intersection number $i_{min}(d, g)$ is independent of genus. On the other hand, a careful examination of the data produced by MICC shows that, for distances 3 and 4, i_{min} depends not only on genus and distance, but also on whether the decomposition in (2) is, at one extreme, into a family of $(4g - 4)$ hexagons or, at the other extreme, into a single $(8g - 4)$ -gon. At this low distance and granular level, we do not yet see hyperbolic behavior emerging.

Here is a guide to this paper and a description of its content. The material in §2 is background for the rest of the paper, consisting of work that is either known or close to known work. In §2.1, we derive equations (2), (3), and (4) above. In §2.2, we review the material that we will need later from [BMM], including efficient geodesics, dot graphs, reference arcs and the surgeries of [BMM] that were performed on intermediate vertices of a path in the curve graph. After that, we will be ready to begin our new work.

In §3, we extend the [BMM] machinery of intersection sequences and dot graphs in the special case when $Dec_{v,w}(S)$ consists only of rectangles and 6-gons. This extension will allow us to perform surgery not only on the intermediate vertices of a path in $\mathcal{C}(S)$, but also on the path’s endpoints.

In §4, we define spirals of rectangles in a decomposition. We prove, in Proposition 4.4, that certain types of surgery are not possible when we restrict ourselves to surgery arcs across the rectangles in $Dec_{v,w}(S)$. We also introduce a new geometric realization of \pm and \mp surgery taken across rectangles, called *spiral surgery*. The main result in this paper is Theorem 4.8, which says that spiral surgery sends efficient geodesics to efficient geodesics, preserving the distance and reducing the intersection number of a geodesic’s endpoints. In effect, Theorem 4.8 tells us that the only way spiral surgery can fail to preserve distance is if it drives the intersection number below the minimum value for the given distance, genus and decomposition.

Acknowledgements: We are grateful for helpful, clarifying conversations with Bill Menasco, Alex Rasmussen, Nick Salter, and Sam Taylor.

2 Background

We begin in the first subsection examining the decomposition $Dec_{v,w}(S)$, connecting it to the study of intersection number and distance in $\mathcal{C}(S)$ and deriving the equations above. The second subsection is a review of the parts of [BMM] that we will use later in the paper.

2.1 The decomposition $Dec_{v,w}(S)$

Let V and E be the number of vertices and edges in the graph induced by $v \cup w$ on S , with $F = |Dec_{v,w}(S)|$ (Note that the vertices and edges in our discussion here about $Dec_{v,w}(S)$ are not vertices in the curve graph). Since every vertex has valence four and every edge touches two vertices, we have $4V = 2E$ or $2V = E$, so that $-2\chi(S_g) = 4g - 4 = 2(-V + E - F) =$

$E - 2F = 2V - 2F$. Therefore:

$$F = F_4 + F_6 + F_8 + F_{10} + F_{12} + \dots \quad (5)$$

But now observe that each edge is an edge of exactly 2 polygons, so that $2E = 4F_4 + 6F_6 + 8F_8 + \dots$ or

$$E = 2V = 2F_4 + 3F_6 + 4F_8 + 5F_{10} + 6F_{12} + \dots \quad (6)$$

where each term on the right and left of equation (6) is non-negative. Combining equations (5) and (6), and noting that $V/4 = i(v, w)$, we obtain equation (3), given in §1.

Note that since every term on both sides of (2) is non-negative, we have learned that the number of possible decomposition vectors (not including rectangles) is finite, and the largest possible polygon in $Dec_{v,w}(S)$ has $8g - 4$ sides. Going back to (6), we then obtain (4).

While the rectangles in $Dec_{v,w}(S)$ do not contribute to Euler characteristic, they do contribute to the number of vertices in the graph $v \cup w$, i.e. to $V = i(v, w)$. In fact, in the special case we consider later, $\{F_4, F_6, F_8, \dots, F_{8g-4}\} = \{F_4, 4g - 4, 0, 0, \dots, 0\}$, the number F_4 of rectangles is given by equation (3) in terms of intersection number $i(v, w)$ and genus g :

$$F_4 = i(v, w) - 6g + 6 \quad (7)$$

Since we already learned that the largest possible polygon in $Dec_{v,w}(S)$ has $8g - 4$ sides and that there are only finitely many possibilities for $F_6, F_8, \dots, F_{8g-4}$, it is clear from equations (3) and (4) that $F_4 \rightarrow \infty$ as $i(v, w) \rightarrow \infty$.

2.2 Background on efficient geodesics

In this section, we define surgery on curves and briefly summarize the relevant background on efficient geodesics that we will need from [BMM]. Given a length d path between two non-separating, filling curves v and w , [BMM] developed a method to reduce the intersections of the *intermediate curves* v_1, v_2, \dots, v_{d-1} in that path. This was accomplished through a collection of simultaneous surgeries on the intermediate curves that left v and w fixed. The authors were able to easily recognize when simultaneous surgeries would preserve pairwise disjointness of v_j, v_{j+1} for each intermediate pair in the geodesic from v to w . This was accomplished by graphing the intersections of the intermediate curves with reference arcs, called the *dot graph*, which we define and generalize.

We begin by recalling the definitions and constructions we will need from [BMM], where the work of finding efficient paths was transformed into questions about sequences of numbers. These sequences represent the intersections of intermediate curves with reference arcs (defined below), and the key breakthrough in [BMM]'s algorithm was using the sequences to make a path efficient.

Definition 2.1. Let P_{2k} be a polygon in the decomposition $Dec_{v,w}(S)$, $k \geq 3$. A *reference arc* α (relative $v \subset \partial P_{2k}$) is an arc that joins two v -sides of P_{2k} .

See Figure 2 for examples of reference arcs. The collection of all possible reference arcs is the union of all reference arcs over all polygons in the face decomposition $Dec_{v,w}(S)$, $k \geq 2$. Note that it is only in the 4-gons and the 6-gons that all of the reference arcs are parallel to the arcs of w , a fact that we will require later.

Definition 2.2. Choose (v, w) with $d = d(v, w) \geq 3$. Let

$$\mathfrak{G} : v = v_0 \rightarrow v_1 \rightarrow \dots \rightarrow v_{d-1} \rightarrow v_d = w \quad (8)$$

be a shortest path from v to w . Assume that v_1 and the reference arcs have been chosen so that v_1 intersects each reference arc minimally. Then \mathfrak{G} is *initially efficient* if v_1 meets each reference arc in the decomposition $Dec_{v_0, v_d}(S)$ at most $d - 1$ times.

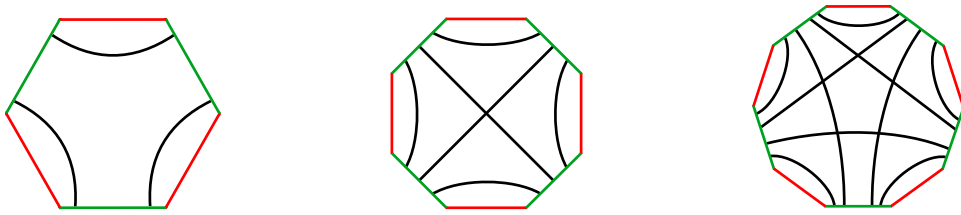


Figure 2: Examples of reference arcs (relative to v), when $k = 3, 4, 5$. The reference arcs are colored black, v is colored green, and w is red.

Definition 2.3. A geodesic \mathfrak{G} is *efficient* if the oriented sub-geodesic v_k, \dots, v_d is initially efficient for each $0 \leq k \leq d-3$ and the oriented geodesic $v_d, v_{d-1}, v_{d-2}, v_{d-3}$ is also initially efficient.

The following finiteness statement from [BMM] will be critical to our work:

Theorem 2.4 ([BMM]). *Let $g \geq 2$. If v and w are vertices of $\mathcal{C}(S)$ with $d(v, w) \geq 3$, then there exists an efficient geodesic from v to w . Additionally, there are finitely many efficient geodesics from v to w .*

We will denote the finite set of efficient geodesics in $\mathcal{C}(S)$ from v to w by $\{\mathfrak{G}_1, \mathfrak{G}_2, \dots, \mathfrak{G}_N\}$.

Definition 2.5. Given a simple closed curve α and an arc γ whose endpoints lie on α (and whose intersection with v is only those endpoints), *surgery on α with surgery arc γ* consists of gluing one of the two components of $\alpha - \partial\gamma$ to γ and discarding the other component of $\alpha - \partial\gamma$. The choice of component to glue to γ is made such that the resulting curve is closed.

Surgeries in [BMM] were categorized by whether the joined arcs are above (+) or below (-) the surgery arc γ , as shown in Figure 3. We will categorize surgeries the same way. The + and - labels in the types of surgery are independent of the orientation of the curves.

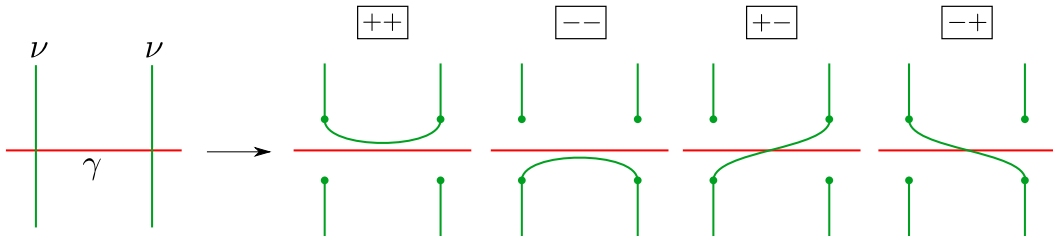


Figure 3: Types of surgery on v with surgery arc γ , as defined in [BMM].

Definition 2.6. Let \mathfrak{G} be an efficient path between v and w , w^k an arc of w , and γ^k a reference arc parallel to w^k . Following the construction in [BMM], we let v_1, v_2, \dots, v_{d-1} be vertices of \mathfrak{G} , and let N_k denote the cardinality of $\gamma^k \cap (v_1 \cup v_2 \cup \dots \cup v_{d-2})$. Traversing γ^k in the direction of some chosen orientation, we record the sequence of natural numbers $\sigma = (j_1, j_2, \dots, j_{N_k}) \in \{1, \dots, d-2\}^{N_k}$ such that the i^{th} intersection point of γ^k with $v_1 \cup v_2 \cup \dots \cup v_{d-2}$ lies in v_{j_i} . Then σ is called the *intersection sequence* of γ^k of $\{v_i\}$.

Now we describe generally the dot graphs of [BMM], which allowed for the visualization of the intersection of intermediate curves with reference arcs. For details, see Section 3 of [BMM]. Given an intersection sequence σ of a reference arc γ^k , we can put σ into a special form, *sawtooth form*, via repeated pairwise permutations of adjacent entries. [BMM] showed that putting an intersection sequence into sawtooth form preserves the adjacency of curves in

the path, as long as the permutations are of entries representing curves that already intersect (i.e., entries with difference greater than 1). To be precise, a sequence is in sawtooth form if it satisfies the condition that $j_i < j_{i+1} \Rightarrow j_{i+1} = j_i + 1$ for each j_i . One can graph a sawtooth-form intersection sequence in a standardized way, as a collection of consecutive dots that are then connected by line segments of slope 1:

Definition 2.7. A *dot graph* is a visual representation of the intersection sequence of γ^k obtained by graphing the intersection sequence as a function $\sigma_k : \{1, 2, \dots, d-2\}^{N_k} \rightarrow \mathbb{N}$. A point (x_i, y_i) of the dot graph represents an intersection of v_{y_i} and γ^k occurring x_i -th along γ^k .

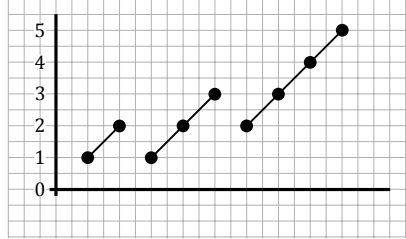


Figure 4: An example of a dot graph. A point (x_i, y_i) of the dot graph represents an intersection of the vertex v_{y_i} in a path and a reference arc γ^k , where the intersection occurs occurring x_i -th along γ^k .

Depending on the heights of the endpoints of two diagonal line segments in a dot graph, we may be able to connect the diagonals with horizontal segments to enclose *regions* of the dot graphs. By region, we mean a box or empty hexagon of type-1 or 2 as defined in [BMM] (see Figure 9 of [BMM]). A region in a dot graph is said to be *pierced* if the interior of a horizontal edge of the region intersects the dot graph, and a region is said to be *empty* if there are no points of the dot graph in its interior.

The first lemma from [BMM] we extend in this paper concerns when one can reduce the intersections of the intermediate curves with the endpoint curve, a step in making the path efficient. The statement in [BMM] is about sequences of numbers and dot graphs representing them. We restate the lemma in the context of the curves and the path they form.

Lemma 2.8 ([BMM] Lemma 3.4, rewritten in the language of curves). *Suppose that σ is an intersection sequence in sawtooth form that has a dot graph with an empty, unpierced box or an empty, unpierced hexagon without an acute exterior angle. Then there is a set of surgeries one can perform on the curves crossing the reference arc of σ such that the result of the surgeries is a path of the same length with fewer intersections of the surgered curves with the reference arc.*

The idea of this lemma is that, when we see empty, unpierced regions in the dot graph, we can perform surgery on each of the curves v_{y_i} that are represented by pairs of dots forming the sides of the region, using a subarc of the reference arc for the surgery arc. See [BMM] for the details, in particular, the very helpful Figure 11. Repeated applications of this lemma make a path efficient while leaving the endpoints fixed. In the next section, we extend the lemma so that we can apply it to the endpoints of a path.

3 Reducing $i(v, w)$ in $\mathcal{C}(S)$

An important note: *we require for the remainder of the paper that $Dec_{v,w}(S)$ consist only of 6-gons and 4-gons.* With this assumption, all reference arcs γ^k are parallel to sub-arcs w^k of

w , see Figure 2. (If we were doing surgery on w instead of v , all the reference arcs would be parallel to arcs of v .) The assumption is necessary because below we will need to examine all possible concatenated pairs of reference arcs, a notion that only makes sense if the reference arcs can be concatenated into a single closed curve. Work is currently underway to generalize the results in these sections to decompositions that include polygons with more than 6 sides.

We begin by defining our construction for a single path \mathcal{P} , then we will apply it to the set of all efficient geodesics from v to w , $\{\mathfrak{G}_1, \mathfrak{G}_2, \dots, \mathfrak{G}_N\}$. Let $\mathcal{P} : v = v_0 \rightarrow v_1 \rightarrow v_2 \rightarrow \dots \rightarrow v_d = w$ be any efficient path between v and w in $\mathcal{C}(S)$.

Definition 3.1 (Extended intersection sequence). Fix a choice of intermediate curves v_i in \mathcal{P} and a pair of consecutive reference arcs γ^k, γ^{k+1} parallel to w (consecutive here means that the arcs of w they are parallel to are consecutive). We concatenate the intersection sequences σ_k and σ_{k+1} of γ^k and γ^{k+1} respectively by adding a 0 to the end of σ_k and joining it to the beginning of σ_{k+1} . We then add a 0 to the beginning of σ_k and to the end of σ_{k+1} . The appearances of 0 in the extended intersection sequence correspond to the three intersections of v with $\gamma^k \cup \gamma^{k+1}$. The sequence of non-negative integers is called an *extended intersection sequence* of a set of vertex representatives v_1, \dots, v_{d-2} along $\gamma^k \cup \gamma^{k+1}$.

We can think of this extended intersection sequence construction as the union of the two intersection sequence functions $\sigma_k : \{1, 2, \dots, d-2\}^{N_k} \rightarrow \mathbb{N}$, and $\sigma_{k+1} : \{1, 2, \dots, d-2\}^{N_{k+1}} \rightarrow \mathbb{N}$ into a single function

$$\sigma_{k,k+1} : \{0, 1, 2, \dots, d-2\}^{N_k + N_{k+1}} \rightarrow \mathbb{Z}_{\geq 0}$$

given by

$$(\sigma_k, \sigma_{k+1}) \rightarrow (0, \sigma_k, 0, \sigma_{k+1}, 0)$$

For example, if the intersection sequences of γ^k and γ^{k+1} were $\sigma_k = (1, 2)$, and $\sigma_{k+1} = (3, 4)$, respectively, then concatenating the intersection sequences above the reference arcs γ^k and γ^{k+1} would give us (in non-sawtooth form) $\sigma_{k,k+1} = (0, 1, 2, 0, 3, 4, 0)$. The permutations of [BMM] extend immediately from sequences of natural numbers to sequences of non-negative integers, so once we have constructed an extended intersection sequence of consecutive arcs γ^k, γ^{k+1} , we can then put the extended sequence into sawtooth form. In the example above, after commuting $\sigma_{k,k+1} = (0, 1, 2, 3, 4, 0, 0)$.

We use extended intersection sequences to include the curve $v = v_0$ in the dot graph:

Definition 3.2 (Extended dot graphs). Starting with the sawtooth-form extended intersection sequence $\sigma_{k,k+1}$, we construct a new dot graph over the joined reference arcs $\gamma^k \cup \gamma^{k+1}$. We call the dot graph of the sawtooth-form extended intersection sequence the *extended dot graph* of $\sigma_{k,k+1}$.

We note that we do not simply concatenate the dot graphs of γ^k and γ^{k+1} . We first put the extended intersection sequence into sawtooth form, and then create the dot graph. Figure 5 shows the individual dot graphs for the sequences $\sigma_k = (1, 2)$, $\sigma_{k+1} = (1, 2, 3, 4)$ and the extended dot graph for the sawtooth-form extended intersection sequence $\sigma_{k,k+1} = (0, 1, 2, 0, 1, 2, 3, 4)$.

Since the extended intersection sequence is in sawtooth form, we can connect vertices with slope-1 and slope-0 edges in the extended dot graph to enclose regions of the plane just as we did with dot graphs. We define the empty and unpierced regions the same way in extended dot graphs just as we did in the original dot graphs. We note that we recognize the degenerate “region” 0,0 in the extended dot graph of an extended intersection sequence of the form $0, \sigma_k, 0, 0$ or $0, 0, \sigma_{k+1}, 0$.

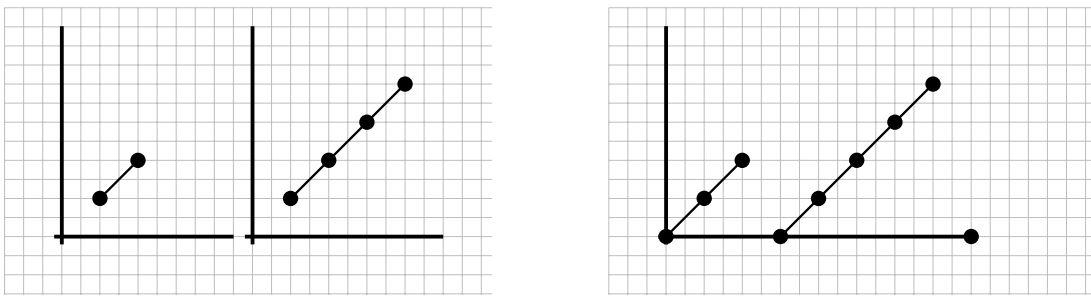


Figure 5: Left: Dot graphs of σ_k, σ_{k+1} . Right: Extended dot graph of $\sigma_{k,k+1}$

There may be no empty, unpierced regions in the dot graphs lying above the individual γ^i for any i . In fact, we assume that is the case: when we start, we may assume that we have already performed as many surgeries on intermediate curves as possible, whenever we found any empty, unpierced regions in any of the individual dot graphs above the γ^k , until all the empty, unpierced regions appearing in any dot graph are removed.

On the other hand, new empty, unpierced regions may appear in the extended dot graph. If the lower corners of such regions are at height > 0 , we are in the situation of [BMM] and we can perform simultaneous surgeries on the intermediate curves comprising the points of the regions. We may assume that as we create extended dot graphs, we remove these regions as they arise. If the lower corners of the regions are at height 0, then simultaneous surgery to remove the region would involve the curve $v = v_0$. In this case, the next lemma, which is an extension of Lemma 3.4 from [BMM], addresses our ability to perform surgery on v and simultaneously on the intermediate curves appearing in the extended dot graph.

Lemma 3.3 (Reducing intersection number of endpoints of a single efficient path). *For an efficient path \mathcal{P} from v to w , suppose that there is a pair of consecutive reference arcs γ^k, γ^{k+1} such that the extended dot graph of the extended intersection sequence $\sigma_{k,k+1}$ has an empty, unpierced box or hexagon. Let v'_i be the result of surgery on v_i along a surgery arc parallel to γ^k , $i = 0, 1, 2, \dots, d-1$ (if $v_i \cap \gamma^k = \emptyset$, then $v'_i = v_i$). Then surgery transforms the path \mathcal{P} into a new path \mathcal{P}' from v' to w , $\mathcal{P}' = (v', v'_1, \dots, v'_{d-1}, w)$, with $i(v', w) \leq i(v, w)$ and the length of \mathcal{P} the same as the length of \mathcal{P}' .*

Proof. The presence of an empty, unpierced region in the extended dot graph implies that if we perform surgery on v along γ^k , we can follow the methods of [BMM] to simultaneously perform surgery on each of the v_{j_i} , where $j_i \in \sigma_{k,k+1}$ appears as a point in the boundary of the region. In particular, our choice of the surgery on v will determine the surgeries on the rest of the curves appearing in the region, following the directed graph in Figure 12 of Lemma 3.4 of [BMM].

All of the surgeries preserve or reduce intersection number; by construction, no new intersections are created. Therefore $i(v', w) < i(v, w)$. Moreover, surgery preserves essentialness. We conclude that the resulting set of curves $v'_1, v'_2, \dots, v'_{d-1}$ represent a path \mathcal{P}' from v' to w in the curve graph of length d . \square

In Lemma 3.3, we do not claim that if \mathcal{P} were a geodesic between v and w then \mathcal{P}' would also be a geodesic, because the surgery indicated by the extended dot graph over \mathcal{P} may reduce the distance from v' to w . Here is why: Lemma 3.3 only explains what is happening in *one* efficient path \mathcal{P} . That is, the extended dot graph only tells us where we might do surgery on v and simultaneous surgeries on the $v_k \in \mathcal{P}$ that result in $i(v', w) < i(v, w)$ and preserve a length d path $v' \rightarrow v'_1 \rightarrow v'_2 \rightarrow \dots \rightarrow v'_{d-1} \rightarrow w$ from v' to w in $\mathcal{C}(S)$ where $d(v'_i, w) = d(v_i, w)$. However, changing the vertices v, w to a new pair v', w affects *every* efficient geodesic with

endpoints v, w . For some other efficient geodesic \mathfrak{G}_r , the extended dot graph above the same pair of reference arcs might have no empty regions. Performing surgery on v along those reference arcs then will produce a path \mathfrak{G}'_r from v' to w with length shorter than \mathfrak{G}_r . Thus showing that a surgery on v preserves $d(v, w)$ requires us to show that (1) the surgery preserves the length of *every* efficient geodesic from v to w that is transformed into a path from v' to w and (2) doesn't create any new, shorter paths between v' and w in $\mathcal{C}(S)$.

We defined the extended dot graph for any efficient path in $\mathcal{C}(S)$, but to consider the extended dot graph for every efficient geodesic, we will need to use the finiteness of the number of efficient geodesics.

Definition 3.4 (Stacked extended dot graph). Since the same curves v, w are the endpoints of each geodesic \mathfrak{G}_i , with the same reference arcs γ^k parallel to the same w -arcs of w , the extended dot graph of adjacent reference arcs γ^k, γ^{k+1} is defined for each of the N efficient geodesics $\{\mathfrak{G}_1, \mathfrak{G}_2, \dots, \mathfrak{G}_N\}$. We can arrange that the placement of the 0's in the extended dot graph (where v crosses the w -arcs) are the same distance apart along the reference arcs (here we mean distance in the usual Euclidean sense, not in the sense of the curve graph). To be precise, we could take the points 0 to be distance $r + 1$ apart along the joined reference arcs, where

$$r = \max_{\mathfrak{G}_m} \{r : v_r \cap (\gamma^k \cup \gamma^{k+1}) \neq \emptyset, v_r \in \mathfrak{G}_m\}.$$

We can then line up the 0's of the $\gamma^k \cup \gamma^{k+1}$ and “stack” copies of all N of them in the direction orthogonal to the planes of the dot graphs. This 3-dimensional graph is the *stacked extended dot graph* of γ^k, γ^{k+1} for the pair of curves v, w , which we will denote $Dot_k(v, w)$. Since the labeling of the arcs of w is cyclic, the stacked extended dot graph $Dot_{i(v,w)}(v, w)$ is the collection of extended dot graphs of $\gamma^{i(v,w)}, \gamma^1$.

Definition 3.5 (Regions in stacked extended dot graphs). Let $Dot_k(v, w)$ be a stacked extended dot graph above γ^k and γ^{k+1} . If there is an empty, unpierced region in the extended dot graph of $\sigma_{k,k+1}$ for each $\mathfrak{G}_i \in \{\mathfrak{G}_1, \mathfrak{G}_2, \dots, \mathfrak{G}_N\}$, then we say that there is an *empty, unpierced region* in $Dot_k(v, w)$.

In Figure 6, we have sketched a simplified example of $Dot_k(v, w)$ for four different paths.

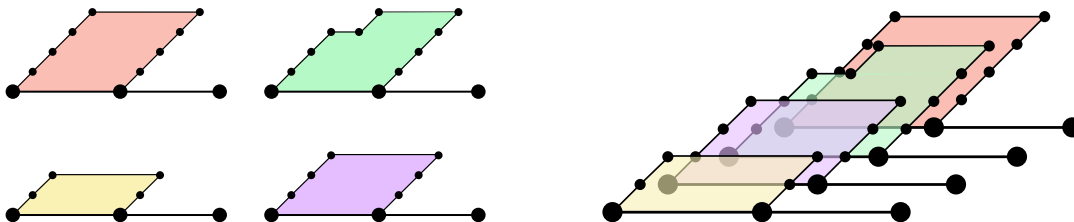


Figure 6: Left: extended dot graphs of $\sigma_{k,k+1}$ for four different paths from v to w . Shaded in for each is an empty, unpierced region. Right: $Dot_k(v, w)$, the stacked extended dot graph for the four paths.

With the guidance of the stacked extended dot graph $Dot_k(v, w)$, we can perform simultaneous surgeries on all of the efficient geodesics between v and w as indicated by the presence of an empty, unpierced region above the surgery arc w^k . Iterating Lemma 3.3, we see that the result will be a set of efficient paths from v' to w of the same length as the distance from v to w . We now consider what more we need to know about surgery to know that $d(v', w) = d(v, w)$.

4 Spiral surgery

In this section, we introduce a new geometric realization of the \pm and \mp surgeries from [BMM] reviewed in Section 2.2, which we call *spiral surgery*. Understanding the decomposition $Dec_{v,w}(S)$ when it contains a certain pattern, called a *spiral*, can predict what the stacked extended dot graph $Dot_k(v,w)$ will look like, which provides a simple condition for this type of surgery to preserve distance.

4.1 A motivating example

Figure 7 depicts two pairs of curves, (v, w) on the left and (v', w) on the right, that are distance 3 in $\mathcal{C}(S_2)$ from w . The curve pairs differ only by the green curve v “wrapping around” and intersecting the red curve w one extra time. We have chosen an arbitrary orientation for our curves and labeled the arcs of the two curves cyclically between their intersection points.

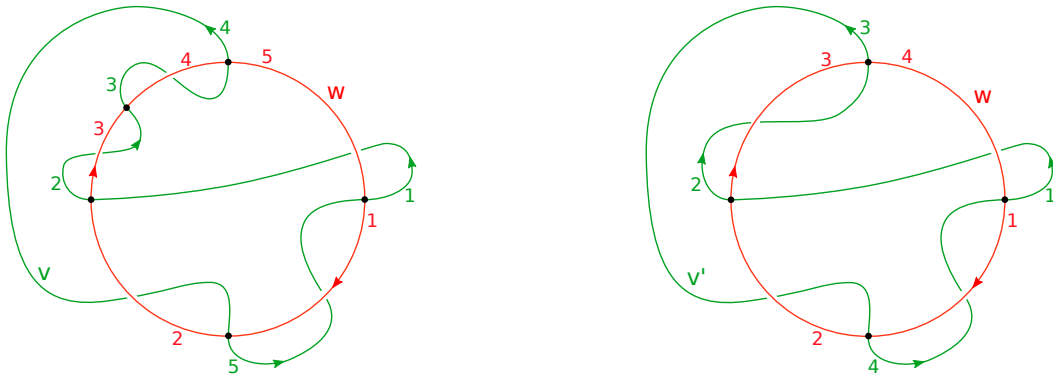


Figure 7: Left: a simple curve pair (v, w) with a spiral; Right: the curve pair (v', w) produced from a \mp surgery on v .

In Figure 7, (v', w) is the result from a \mp surgery relative to the arc w^3 on (v, w) . To be precise, we cut open v at two consecutive intersection points of v^2 with w (recall that v^2 is the arc in v labeled 2 in Figure 7) and replace v^2 with a parallel copy of the surgery arc w^3 . After relabeling so that arcs of v are still consecutive, we have the curve pair on the right. In Figure 3, we saw that, generally, \mp surgery reduces the intersection number of v with its surgery arc by 1. For this figure’s simple interpretation of a \mp surgery, we see also that the intersection number of the curve pair (v, w) is also reduced by 1, since the bit of v deleted by surgery only intersects w along the surgery arc w^3 . The fact that both curve pairs are distance 3 follows from the fact that both pairs fill S_2 and have intersection number far below what is required for distance 4 on S_2 .

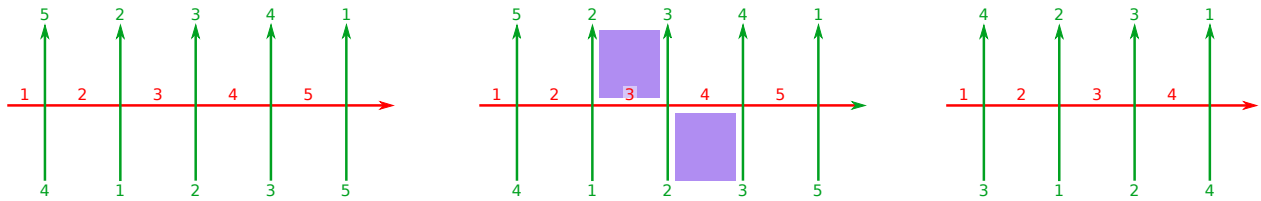


Figure 8: Menasco ladder representations of (v, w) and (v', w) from Figure 7. The shaded rectangle was removed when v^3 was deleted in the left figure.

While cyclic embeddings like those of Figure 7 are visually appealing, they are impractical for computations relevant for this discussion. We need a straightforward representation of

curve pairs that allow for easy visual inspection of $Dec_{v,w}(S)$. Our preferred choice is the *Menasco ladder*, first defined in [GMMM]. It presents pairs of curves in a tabular form, using the labels of the arcs from the cyclic representation above. The Menasco ladder is the primary way of inputting the curves into MICC for analysis; input consists of two n -vectors, one for the top labels of v , and one for the bottom. To produce a Menasco ladder from a cycle as in Figure 7, we first cut open w and lay it horizontally, such that w^1, \dots, w^n are listed sequentially. Each arc of v is then split between each intersection point. Identifying labels of split arcs allows us to recover the original curves quickly.¹ The effect of this simple \mp surgery on the decomposition of (v, w) is the deletion of a single rectangle. Identifying the rectangle in Figure 7-left from the cyclic representation is very difficult, even in this simple example. However, the rectangle is easily recognized in the Menasco ladder as a repeated sequence of numbers 2, 3 in the top labels and the bottom labels. As shown in Figure 9-left, the identified corners of the rectangle in the decomposition of (v, w) means that the rectangle is wrapped around a handle of the surface. When this wrapped rectangle is projected into the plane, a spiral is evident. Notice the equivalence of the planar projection in Figure 9-right and the portion of the Menasco ladder in Figure 8 containing the rectangle.

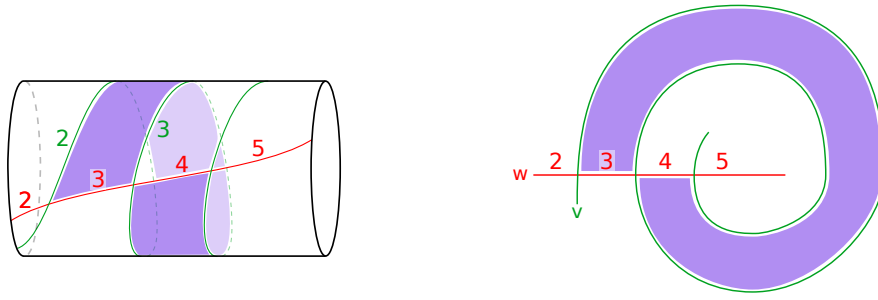


Figure 9: Representing a rectangle as a spiral

4.2 Spirals

We assume in this section that we have cut the closed surface open along v , producing a surface with two boundary components crossed by arcs of w . We note that all of the arguments hold if instead we cut the surface open along w and interchange the roles of v and w everywhere. Our first step is to formalize the rectangle pattern in the Menasco ladder observed in the example above.

Definition 4.1 (Bands, length, width). A v -band of 4-gons \mathcal{B}_v in $S - v$ is a sequence of one or more 4-gons in $Dec_{v,w}(S)$ that are identified along w -edges, with its initial and final 4-gons attached along w -edges to $2k$ -gons, $k > 2$. Note that the v portion of $\partial\mathcal{B}_v$ consists of two ‘long’ edges, each a subsequence of the cyclically ordered edges of v . The v -length of \mathcal{B}_v is the number of consecutive v -edges in $\partial\mathcal{B}_v$. By construction, the length of a band is the number of 4-gons in \mathcal{B}_v . The v -width of \mathcal{B}_v is $\min\{m_v, i(v, w) - m_v\}$, where m_v is the absolute value of the difference between the labels on the v -edges of any 4-gon in \mathcal{B}_v .

If there is no confusion, we will simply refer to a v -band \mathcal{B}_v , as a 4-gon *band* \mathcal{B} and the v -length and v -width of \mathcal{B}_v as the *length* and *width* of \mathcal{B} . It is simple to see that v -length and m_v (and hence, v -width) are independent of the choice of labeling and the choice of 4-gon

¹The reader may wish to check their understanding of Menasco ladders by showing that the ladder with top edges 1, 5, 9, 3, 2, 6, 10, 4, 7, 6 and bottom edges 10, 4, 8, 2, 1, 5, 9, 3, 8, 7 determines the example that was given earlier in the left sketch of Figure 1. It has genus 2 and distance 3. MICC tells us that its decomposition has $F_4 = 4$ and $F_6 = 4$.

along which they are computed, because the gluing of the two boundary components of $S - v$ determines labelings up to cyclic permutation.

Definition 4.2 (Spirals). A v -spiral in $S - v$ (or *spiral*, when not ambiguous) is a v -band with identified v -edges that intersects one or more consecutive edges of w . The *width* and *length* of a v -spiral is the width and length of the v -band comprising it.

Definition 4.3 (Spiral interior). The *interior* of a spiral is the set of rectangles that are bounded on all four sides by other rectangles in the spiral. The *barrier* rectangles of a spiral are those that are not in the interior of the spiral.

In Figure 10-right, the barrier rectangles are shaded yellow. In Figure 10-left, which has length 14 and width 5, the interior of the spiral is a single loop. One can recognize spirals in the Menasco ladder notation introduced earlier in this section the same way that one recognizes single rectangles: as sequences of numbers that appear in both the top and bottom vectors of the ladder.

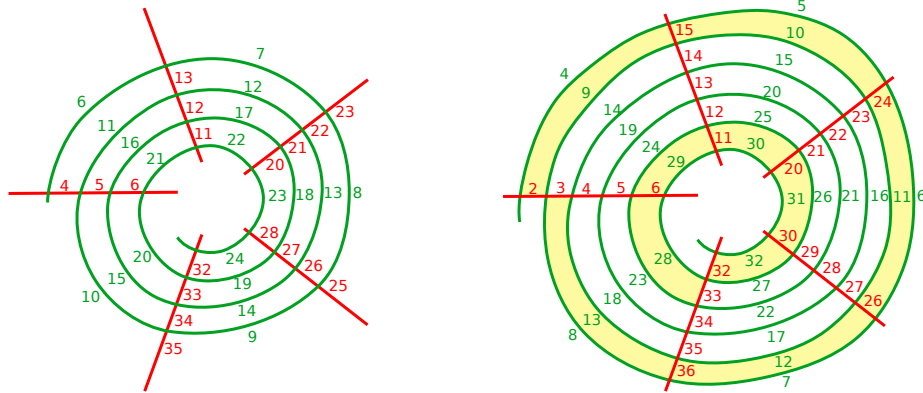


Figure 10: Left: A v -spiral as a planar projection of a 4-gon v -band wrapping around S . It has length 14 and width 5. Right: An example of a spiral winding in the opposite direction, with the barrier rectangles shaded. It has length 24 and width 5.

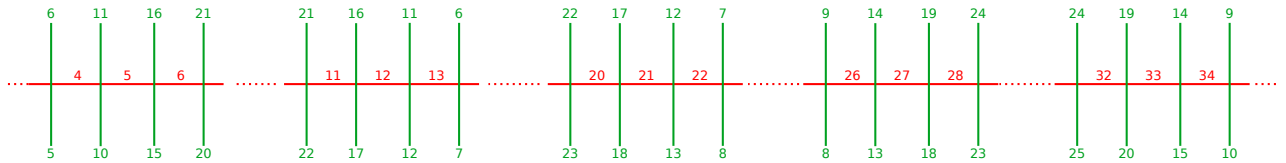


Figure 11: Detail from the Menasco ladder of the spiral from Figure 10-left.

Suppose we have a pair of vertices in $\mathcal{C}(S)$ with very large $i(v, w)$. We know that, thanks to the equations in Section 2.1, the number of $2k$ -gons $k > 2$ is finite in $Dec_{v,w}(S)$, so large intersection numbers will be manifested by a large number of 4-gons in $Dec_{v,w}(S)$. As $F_4 \rightarrow \infty$, there is no way to configure the decomposition that prevents the formation of bands. This means that we can expect to see some form of spiraling as $i(v, w)$ gets large and, conversely, any surgery to reduce intersection number should naturally take place along these bands. It is possible that multiple bands will form spirals together, as in Figure 12.

4.3 Spiral surgery

Before examining how spirals guide the reduction of intersection number and the removal of rectangles, we make a preliminary observation. In Figure 3, which was taken from [BMM],

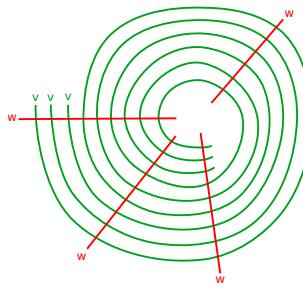
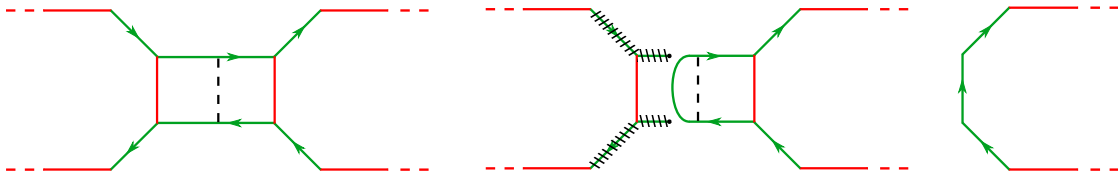


Figure 12: A 3-spiral, a spiral consisting of three 4-gon bands.

there were 4 types of surgery: $++$, $--$, \pm and \mp . In our work, we discovered that when we perform surgery on v or w across rectangles in $Dec_{v,w}(S)$, if we want to preserve the distance between v and w , then we are limited to \pm and \mp surgery.

Proposition 4.4. *Let $v, w \in \mathcal{C}(S)$ be such that $d(v, w) \geq 3$. Let γ be a reference arc contained in a rectangle in $Dec_{v,w}(S)$. Then type $++$ or $--$ surgery on either v or w relative to the surgery arc γ will not preserve $Dec_{v,w}(S)$.*

Proof. Consulting Figure 3, we see that, if we are performing $++$ or $--$ surgery across a rectangle, the two strands of the to-be-surgered curve v in the leftmost sketch of Figure 3 must have opposite orientations and the result of surgery will be a choice of one of two simple closed curves. Without loss of generality, suppose that we performed a surgery of type $++$ across γ in a rectangle r that is part of a band of ≥ 1 rectangles joining w -edges 6-gons $P, Q \in Dec_{v,w}(S)$, where it is possible that $P = Q$. Figure 13-left depicts the setup.

Figure 13: $++$ or $--$ surgery that preserve $Dec_{v,w}(S)$ do not occur.

After the surgery, v will be changed to two distinct closed curves, v' and v'' and (without loss of generality) we choose one of them, say v' , so our new pair is (v', w) . We will show that (v', w) does not fill S . Figure 13-middle shows v' and focuses on the polygon P . The surgery creates a bigon in (v', w) and, after pushing v' across the bigon, there will be a new bigon if there is another rectangle in the band, and the argument can be repeated. We continue to push v' across the rectangles to eliminate bigons. The final bigon will be formed by v' and an w edge of P . After removal of this final bigon the polygon P will have changed to a polygon P' with 2 fewer edges. Thus F_4 has increased by 1 and F_6 has decreased by 1, while no other polygons have been created. However, (v', w) cannot be a filling pair, by the equations in Section 2.1, so our surgery of type $++$ could not have occurred. \square

Definition 4.5 (Spiral Surgery). Let \mathcal{B} be a v -spiral. *Spiral surgery* is a \pm - or \mp -surgery on v relative to one w -edge in \mathcal{B} .

See Figure 14, where we have chosen a w -arc at 9 o'clock for our surgery arc. The surgery is standard \pm or \mp surgery: one piece of v in the spiral that begins and ends on the endpoints of the surgery arc is removed, then replaced with a parallel copy of the surgery arc, leaving v otherwise unchanged. The advantage of spiral surgery is that the arc of the curve to be

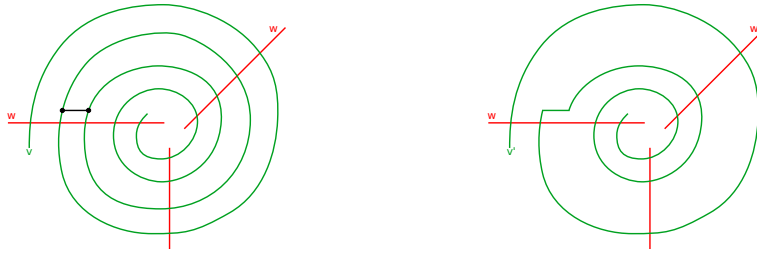


Figure 14: An example of spiral surgery across a single 4-gon. Left: a spiral in a curve pair (v, w) , in green and red respectively, and the surgery arc in black. Right: The resulting curve pair (v', w) after spiral surgery.

deleted is completely contained within the spiral. This localizes the effect of a \pm/\mp surgery to the spiral, allowing us to analyze the new curve.

The sign of the spiral surgery (whether it is \pm or \mp), is determined only by the direction the spiral winds on the surface, independent of orientation. One direction of winding results in \pm -surgery, while the other direction of winding only allows for \mp surgery. See Figure 10.

What is the effect of spiral surgery on $i(v, w)$ and the decomposition $Dec_{v,w}(S)$? Spiral surgery removes several 4-gons from the 4-gon band comprising the spiral; the number of 4-gons removed is equal to the width of the spiral. All other 4-gon bands are left fixed and the number and type of $2k$ -gons in the decomposition, for $k > 2$, is unchanged. Spiral surgery reduces $i(v, w)$ by the width of the spiral, so the width of a band gives us critical initial information: our first check for when a spiral surgery preserves distance in the curve graph.

Proposition 4.6. *Let \mathcal{B} be a v -spiral in $S_g - v$. Let m be the width of \mathcal{B} and let i_{min} be the minimum intersection number for the given genus, distance, and equivalence class of $Dec_{v,w}(S)$. If the width of the spiral is greater than $i(v, w) - i_{min}$ then spiral surgery along \mathcal{B} reduces the distance between v and w in $\mathcal{C}(S)$.*

Proof. The claim follows immediately from the preceding discussion. □

4.4 When does spiral surgery preserve distance?

The main result in this section is Theorem 4.8, at the end of this section. It says that, under certain conditions, the only way that spiral surgery fails to preserve distance is if it reduces the intersection number below $i_{min}(d, g)$.

The identification of the v -arcs of a v -spiral places strong constraints on the dot graphs over any reference arcs parallel to the w -arcs in the spiral. The constraints are so strong, in fact, that we can prove the following lemma.

Lemma 4.7. *Let $\mathfrak{G} : v = v_0 \rightarrow v_1 \rightarrow \dots \rightarrow v_{d-1} \rightarrow v_d = w$ be an efficient geodesic between v and w , with $d \geq 3$, and suppose that there is a spiral on $S - v$. After possible distance-preserving isotopy of the v_j , all of the reference arcs in the interior of the spiral have either the same dot graph or the dot graph resulting from the reversed sequence. Thus the dot graphs in a spiral are all the same.*

Proof. If the dot graphs were different for some reference arcs in the interior of the spiral, then there would be a v_i entering and exiting the spiral that intersects only some of the spiral's reference arcs.

If v_{d-1} entered the interior of the spiral, then it could cross one of the “spokes”, an arc of $w = v_d$, but that is impossible since v_{d-1} and v_d are disjoint. Instead, v_{d-1} must cross v

twice without crossing w , resulting in a bigon. However, we ruled out bigons by assuming our curves intersect minimally. Thus there can be no appearance of v_{d-1} in the interior of the spiral. If $d > 3$, it is possible that v_{d-2} enters and exits the interior of the spiral. We could simply isotope it across v and move it off the spiral entirely, since v and v_{d-2} already intersect, unless there is a v_{d-3} traveling alongside v_{d-2} . Now if $d-3 > 2$, we could isotope the pair v_{d-2} and v_{d-3} across v simultaneously and move them both away from the interior of the spiral. The obstacle to doing that isotopy is if there is a v_{d-4} traveling alongside the v_{d-3} that the v_{d-3} must stay disjoint from, and so on. This argument continues for successive v_{d-k} until $d-k=2$, when we reach the following conclusion: either there is a v_1 in the interior of the spiral, which forces the entire sequence $v_2, v_3, \dots, v_{d-3}, v_{d-2}$ to travel along the entire length of the interior of the spiral, or there is no v_1 so we can remove any entering/exiting collection of curves $v_r, v_{r+1}, \dots, v_{d-2}$ (for $2 \leq r < d-2$) by simultaneous isotopy across v . For, since we have assumed minimal position, we can assume that v_1 either does not appear in the spiral at all or it travels the entire length of the interior of the spiral, parallel to v . If every reference arc in the spiral is intersected by the same curves, arranged in the same order with respect to each reference arc, then by definition, the intersection sequences are the same. Thus the dot graphs are the same. \square

There are implications in this lemma for the set of simultaneous surgeries on the intermediate vertices of an efficient path that are induced by the spiral surgery on the endpoint v . We ruled out $++$ and $--$ surgery across rectangles in Proposition 4.4, so we know that the only possible intermediate surgeries indicated by the surgery arc in spiral surgery are of type \pm and \mp . It follows that the type of spiral surgery on v is the same as the type on every intermediate curve that appears in the interior of the spiral and that the deleted arc of each surgered v_k is the arc parallel to the deleted arc of the surgered v . Moreover, Lemma 4.7 tells us that the only intersections of intermediate curves v_i, v_j in the interior of the spiral would be an even number of crossings, resulting in bigons that could all be removed. After isotopy, the set of intermediate v_i 's in the interior of the spiral are disjoint and parallel to v . Spiral surgery does not affect intersections of v_j with v_i , it will only reduce intersections of v_j with w . To summarize, we understand the effects of a spiral surgery not only on the endpoints of a path but also of the induced simultaneous surgery on all the intermediate curves in the path.

Recall that i_{\min} was defined in Section 1 to be the minimal intersection number taken over all choices of vertices $v, w \in \mathcal{C}(S_g)$ having distance d and having a given equivalence class of decomposition. This number can, in principle, be determined algorithmically by the techniques that were used in [BMM] to enumerate efficient geodesics, but applied now to the endpoints as well as the interiors of efficient geodesics. At the time of this writing, we only know it explicitly for various equivalence classes of decompositions when $(d, g) = (3, g)$ and $(d, g) = (4, 2)$.

Theorem 4.8 (Spiral surgery preserves efficiency and distance). *Let v, w be vertices in $\mathcal{C}(S)$, S closed and genus g , with distance $d = d(v, w) \geq 3$. Let $\text{Dec}_{v,w}(S)$ consist of all 4-gons and 6-gons, and suppose that $\text{Dec}_{v,w}(S)$ has a v -spiral of width m and there is an empty, unpierced region in $\text{Dot}_k(v, w)$ over the interior of the spiral. Let v' be the result of the indicated spiral surgery on v . Let $\{\mathfrak{G}_1, \mathfrak{G}_2, \dots, \mathfrak{G}_n\}$ be the set of all efficient geodesics connecting v and w in $\mathcal{C}(S)$ and let $\{\mathfrak{G}'_1, \mathfrak{G}'_2, \dots, \mathfrak{G}'_n\}$ be the set of paths resulting from the simultaneous surgeries on each \mathfrak{G}_j as indicated by each extended dot graph. Then $i(v', w) < i(v, w)$ and each \mathfrak{G}'_j is an efficient path of length $d(v, w)$ from v' to w . Furthermore, $d(v', w) = d(v, w)$.*

Proof. Each \mathfrak{G}'_j is a path of length d , due to repeated applications of Lemma 3.3.

We recall that a path is efficient if the oriented sub-geodesic $v_k, \dots, v_d = w$ is initially efficient for each $0 \leq k \leq d-3$ and the oriented path $v_d, v_{d-1}, v_{d-2}, v_{d-3}$ is also initially efficient.

We assume that we have performed all possible surgeries to remove any empty, unpierced regions in the stacked extended dot graphs and prove the claim by contradiction.

We first check that the first part of the definition holds true for $\mathfrak{G}'_j = v', v'_1, \dots, v'_{d-2}, v'_{d-1}, w$. Fix k . The reference arcs γ' are parallel copies of arcs of w , where the endpoints of the arcs are the intersections of w with v'_k . We know that the original subgeodesic $v_k, v_{k+1}, \dots, v_{d-1}, w$ was initially efficient, so that $|v_{k+1} \cap \gamma| \leq d - k - 1$, where γ was a reference arc parallel to w and disjoint from v_k . If $v'_k = v_k$, then there is nothing to show, so let's assume that $v'_k \neq v_k$. Since w was not changed by surgery, the reference arcs γ' that are parallel to w can only be the union of consecutive reference arcs from the set of those γ considered for the subgeodesic from v_k to w . We note here that since the surgery is a spiral surgery, the decomposition is unchanged, so the $Dec_{v',w}(S)$ still consists of 6-gons and 4-gons. In particular, the reference arcs in the decomposition of the image of the spiral surgery are still parallel to the edges of w , so can be concatenated to allow us to consider the stacked extended dot graph in the images of the set of efficient paths $\{\mathfrak{G}'_1, \mathfrak{G}'_2, \dots, \mathfrak{G}'_n\}$. Thus $|v'_{k+1} \cap \gamma'| \leq m(d - k - 1)$, where m is the number of consecutive reference arcs it takes to build γ' from the γ 's that were reference arcs for the efficient subgeodesic from v'_k to w . Suppose, for the sake of contradiction, that $m > 1$. Then there are repeats in the intersection sequence (which consists of non-negative integers from 0 to $d - k - 1$) over γ' that represents the subpath from v'_k to w . Repeats in the intersection sequence indicate spots where there are surgeries available to reduce the intersection of the intermediate curves, as in [BMM]. However, such surgeries are represented by the presence of empty, unpierced regions in the extended dot graph, contradicting our assumption that we have already performed all of the surgeries needed to reduce the intersections as much as possible among intermediate curves in the path. Thus $m = 1$ and the oriented path $v'_k, \dots, v'_d = w$ is initially efficient for arbitrary k .

Finally, we consider whether the oriented path $w = v_d, v'_{d-1}, v'_{d-2}, v'_{d-3}$ that results from the surgeries is also initially efficient. Since the surgery arcs were all parallel to arcs of w , and since w and v_{d-1} are disjoint, $v'_{d-1} = v_{d-1}$. Combined with the same argument as above, we conclude the new path after surgery is efficient, since the original path $v_d, v_{d-1}, v_{d-2}, v_{d-3}$ is efficient.

Proving that $d(v', w) = d(v, w)$ requires that we show that there is no efficient path from v' to w with length shorter than $d(v, w)$. For the sake of contradiction, let us suppose that there is such a path, so $d(v', w) = d' < d(v, w)$ and let's examine the first of the intermediate curves in the path. That is, we choose $x \in \mathcal{C}(S)$ such that $d(v', x) = 1$ and $d(x, w) = d' - 1$. Such an x has $d(v, x) > 1$, for otherwise there is a path from v to w through x that has length less than $d(v, w)$. Let $\chi \in x$ be a representative curve. The assumption that $d(x, v) > 1$ but $d(x, v') = 1$ means that x and v only intersected along the interior of the spiral. However, this contradicts Lemma 4.7, since the dot graphs on the interior of the spiral would change as χ crosses v . There must be no such x . \square

Theorem 4.8 and Proposition 4.6 tell us that the spiral width and the stacked, extended dot graph above the spiral interior are necessary and sufficient for recognizing when spiral surgery will preserve distance.

5 Conclusion

The basic problem that was studied in this paper is how to reduce intersection number between two curves without reducing distance. The tools that we used were closely related to those in [BMM], where the concept of an *efficient geodesic* joining two vertices in the non-separating curve graph first appeared. In particular, we discovered that certain surgeries that had played a major role in [BMM] lead us in a natural way to the discovery of *spiral surgery*.

In Section 3, we formalized how a surgery can reduce the intersection number between two curves while preserving both the length and the efficiency of a given efficient path between them. Section 4 then applied these results to a specific surgery along sequences of rectangles in $Dec_{v,w}(S)$ and proved that such a surgery can maintain distance in $\mathcal{C}(S)$ while reducing the intersection number.

The proof of Theorem 4.8 provides a new lens through which one can view the local geometry of $\mathcal{C}(S)$. Let (v, w) be a filling pair, and let $\mathfrak{G} = \{\mathfrak{G}_1, \dots, \mathfrak{G}_N\}$ be the efficient geodesics between v and w . Let $\mathbb{S}(\cdot)$ denote the application of a surgery to a curve or set of curves on S . As we've seen here and in [BMM], the operator $\mathbb{S}(v, w)$ implicitly operates on all paths between (v, w) , so for a path $p \subset \mathcal{C}(S)$, we can write $\mathbb{S}(p) = \{\mathbb{S}(c) | c \in p\}$.

Theorem 4.8 establishes a general tool to determine when a surgery preserves efficiency of potential geodesics between (v, w) : the stacked extended dot graph. The key idea is to check the dot graphs of all efficient geodesics that would be affected by \mathbb{S} simultaneously for common empty, unpierced regions. This idea can be used to answer questions about the action of a general \mathbb{S} on (v, w) by studying the action of \mathbb{S} on the dot graphs of efficient geodesics between (v, w) . One can also restrict attention to the action of \mathbb{S} on the set of geodesics \mathfrak{G} and, in particular, the subsets of $\mathbb{S}(\mathfrak{G})$ with length equal to k , $\mathbb{S}_k(\mathfrak{G}) = \{\mathfrak{G}_i | |\mathbb{S}(\mathfrak{G}_i)| = k\}$.

We consider when \mathbb{S} strictly decreases or increases the distance between (v, w) : $\mathbb{S}(\mathfrak{G}) = \bigcup_{k=1}^{d(v,w)-1} \mathbb{S}_k$ or $\mathbb{S}(\mathfrak{G}) = \bigcup_{k=d(v,w)+1}^{\infty} \mathbb{S}_k$, respectively. We now know that, in the case of spiral surgery, the former occurs when the assumptions of Theorem 4.8 are violated. Regarding the latter, Aougab and Taylor provide an algorithm to construct an infinite geodesic ray, also using repeated applications of Dehn twists [AT]. At each step of the algorithm, a geodesic is produced that is strictly longer than the previous one. We conjecture that a surgery-based algorithm of a similar flavor exists, using our machinery of $Dec_{v,w}(S)$ and efficient geodesics. Let's explore this idea, first from the perspective of $Dec_{v,w}(S)$.

Figure 15-left is a genus 2 surface cut open along a green curve v that is distance 3 from red curve w . It is identical to that in Figure 1. In Figure 15-right, the same surface is cut open along a modified green curve v' paired with the same red curve w . The difference between the surfaces $S - v$ and $S - v'$ is that there are two additional rectangles in $S - v'$ marked by edges of w between the 6-gons. The distance between v' and w is 4 (confirmed by MICC). We got from v to v' by performing two operations, each the inverse of a spiral surgery, a transformation we call *spiral addition*. This spiral addition is related to the tools used in [AT], where the growth of the minimum intersection number between vertices in the curve graph with distance and genus was studied. It is also related to the tools used in [PS] and most recently [Ras], where the hyperbolicity of the non-separating curve graph was studied with an emphasis on the techniques of combinatorial topology.

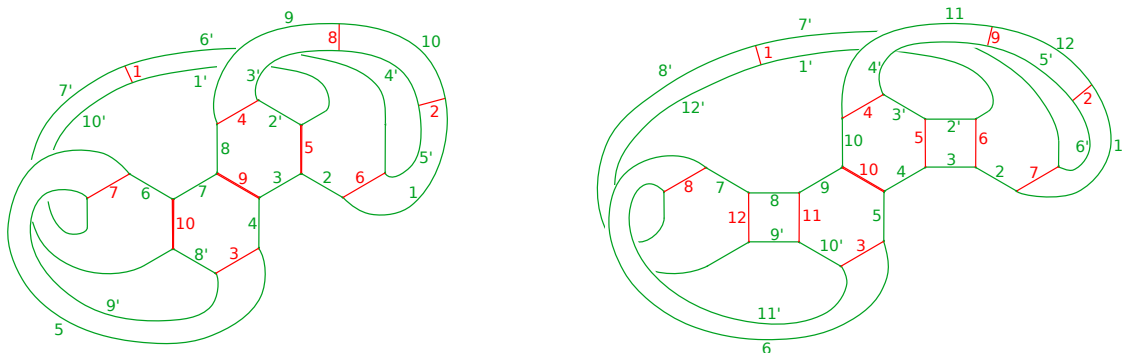


Figure 15: Left: a genus 2 surface cut open along a green curve distance 3 from the red curve. Right: same surface cut open along a curve distance 4 from the same curve.

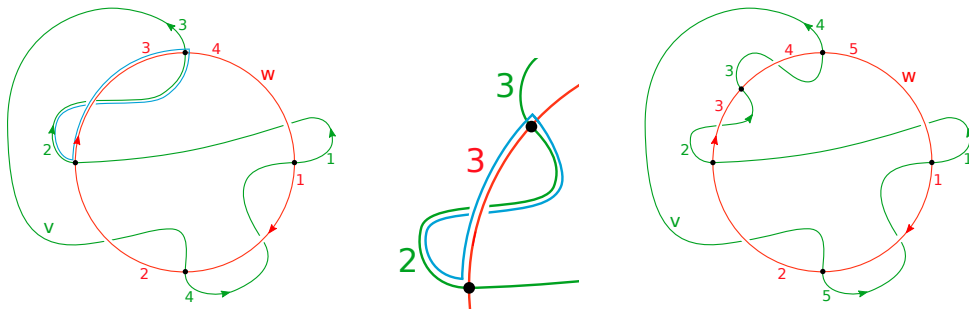


Figure 16: The transformations of curve pairs from left to right are given by spiral addition

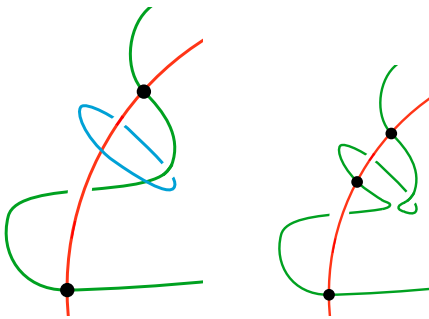


Figure 17: The realization of spiral addition by a Dehn twist of the green curve v' about the blue curve.

To explain the connection, let's return to the example in §4.1. See Figure 16, where we have reversed the order of the two sketches in Figure 7, and added a new sketch in the middle. Recall that filling pairs such as the curves v (in green) and w (in red) intersect many times and so determine in a natural way a collection of *bicorn curves* [PS, Ras]. A bicorn curve is a curve formed from the filling pair $v \cup w$ as the union of two simple arcs, one a subarc of v' and the other a subarc of w , where the arcs intersect only at their endpoints. In the example in Figure 16 the bicorn, shown in red and green, is formed from arc 2 of v' and arc 3 of w in the left sketch. Its push-off from v and w into the interior of the positively oriented surface S , which we denote β , intersects v' once, and in the figure is blue. Figure 17 shows that v is the image of v' under a Dehn twist T_β about the push-off β of the bicorn. Thus, the addition of an m -rectangle spiral will replace v' with $T_\beta^m(v')$, relating our work to the methods used in [AT] to extend a given geodesic.

The example in Figure 15 above was constructed similarly. In Figure 15-left, there are two bicorn curves whose push-offs we perform simultaneous Dehn twists around: red 5 \cup green 2, and red 10 \cup green 7. A bicorn curve in the decomposition can be recognized by the same color edge meeting both ends of the other color edge. Using these bicorns to increase the distance as in these examples only works to take us from distance 3 to distance 4, though. That is, these simple additions won't get the curves any further apart in the curve graph. This is because the bicorn curve in these examples intersects each of v' , v , and w once, so it is always distance 2 from each. We conjecture that there is a generalization of this spiral surgery that will lead to a distance-increasing algorithm that is as well-controlled as spiral surgery is.

All this is to say that (i) spiral reduction and spiral addition are closely related problems, and (ii) connections exist between our work and the problems solved in [AT] and [PS], where Dehn twists along generalized bicorns are the primary tools for creating paths between vertices in the curve graph, and extending geodesics to longer ones. Work is in progress on both of

these problems.

References

- [AT] Aougab, T., Taylor, S.J.: Small intersection numbers in the curve graph. *Bull. Lond. Math. Soc.* 46(5), 989-1002 (2014) arXiv:1310.4711
- [BM] Birman, J. and Menasco, W. The curve complex has dead ends *Geom Dedicata* **177** (2015) 71-74. arXiv:1210.6698
- [BMM] Birman, J., Margalit, D., and Menasco, W. Efficient geodesics and an effective algorithm for distance in the complex of curves, *Math. Ann.* **366** No. 1 (2016) 1253-1279. arXiv:1408.4133
- [GMM] Glenn, P., Menasco, W., Morrell, K., and Morse, M. MICC: A tool for computing short distances in the curve complex, *J. Symb. Comp.* **78** (2017) 115-132. arXiv:1408.4134
- [He] Hempel, J. *3-manifolds as viewed from the curve complex*, *Topology* **40** (2001) 631-657. arXiv:math/9712220
- [Lea] Leasure, J.P.: Geodesics in the complex of curves of a surface. ProQuest LLC, Ann Arbor. Thesis (Ph.D.), The University of Texas, Austin (2002)
- [MICC] Glenn, P. and Morse, M. *MICC: Metric in the Curve Complex*. Software package and software tutorial are posted for download at <http://micc.github.io>
- [MM-I] Masur, H. and Minsky, Y. Geometry of the complex of curves I: Hyperbolicity *Inventiones Math.* **138(1)** (1999) 103-149. arXiv:math/9804098
- [MM-II] Masur and Minsky, Y. Geometry of the complex of curves II: Hierarchical structure *Geom. Funct. Anal.* **10(4)** (2000) 902-974. arXiv:math/9807150
- [PS] Przytycki, P. and Sisto, A. A note on acylindrical hyperbolicity of mapping class groups. In *Hyperbolic geometry and geometric group theory*, Koji Fujiwara, Sadayoshi Kojima, and Kenichi Ohshika, editors, number 73 in Advanced Studies in Pure Mathematics, 255 - 264. Mathematical Society of Japan, 2017. arXiv:1502.02176
- [Ras] Rasmussen, A. Uniform hyperbolicity of the graphs of nonseparating curves via bicorn curves *Preprint*: arXiv:1707.08283

Joan S. Birman, Department of Mathematics, Columbia University, New York, NY 10027
 <jb@math.columbia.edu>

Matthew J. Morse, Department of Computer Science, Courant Institute for Mathematical Sciences, New York University, New York, NY 10012 <mmorse@cs.nyu.edu>

Nancy C. Wrinkle, Department of Mathematics, Northeastern Illinois University, Chicago, IL 60640 <n-wrinkle@neiu.edu>